Evidence of O-H Bond in the Bulk State of Protonic Conductor Y-Doped SrCeO$_3$ by Soft-X-Ray Spectroscopy

Tohru HIGUCHI, Shu YAMAGUCHI[1], Noriko SATA[2], Shik SHIN[3,4] and Takeyo TSUKAMOTO

Department of Applied Physics, Tokyo University of Science, 1-3 Kagurazaka, Shinjuku-ku, Tokyo 162-8601, Japan
[1]*Department of Materials Science, University of Tokyo, 7-3-1 Hongo, Bunkyou-ku, Tokyo 113-8656, Japan*
[2]*Department of Machine Intelligence and Systems Engineering, Tohoku University, 1 Aoba, Aramaki, Aoba-ku, Sendai 980-8579, Japan*
[3]*Institute for Solid State Physics, University of Tokyo, 5-1-5 Kashiwanoha, Kashiwa, Chiba 277-8581, Japan*
[4]*RIKEN, 1-1-1 Kouto, Mikazuki-cho, Sayo-gun, Hyogo 679-5198, Japan*

The electronic structure in the band-gap region of protonic conductor Y-doped SrCeO$_3$ has been investigated by soft-X-ray emission spectroscopy (SXES) and X-ray absorpiton spectroscopy (XAS), which reflect the electronic structure in the bulk state. The O $1s$ SXES spectrum exhibits three O $2p$ states, which correspond to the top of the valence band, near the Fermi level, and the botttom of the conduction band. The O $1s$ XAS spectrum exhibits the existence of hydrogen structures whose energy positions match with those of the three O $2p$ states. These findings are direct evidence of the O-H bond in the bulk state.
[DOI: 10.1143/JJAP.42.L1265]

It is well known that perovskite-type oxide of general formula ABO$_3$ exhibits protonic conductivity at high temperature when acceptor ions are doped in the B^{4+} ion site.[1–6] This protonic conductor has many promising potential electrochemical applications such as hydrogen sensors and fuel cells.[7] Most attention has been focused on cerates and zirconates because of their excellent protonic conductivity and chemical stability. In particular, Y^{3+}-doped SrCeO$_3$ (SrCe$_{1-x}$Y$_x$O$_{3-\delta}$) has the highest protonic conductivity in a high temperature region. Shin *et al.* measured the proton conductivity using a single crystal of SrCe$_{1-x}$Y$_x$O$_{3-\delta}$.[2] They confirmed that the hydrogen migrates in the bulk, and found, from the isotope effects, that the proton tunneling effect is negligible. In the infrared absorption spectra of O-H stretching, a large absorption band is observed in the wave-number range of $\sim 3200\,\mathrm{cm}^{-1}$, which is assigned to the proton site accompanying a dopant cation. However, these results are not direct evidence that hydrogen exists in the bulk state.

In the perovskite-type protonic conductor, we believed that hydrogen is incorporated by dissolution of H$_2$O through the reaction with an oxygen vacancy and an oxide ion from two O-H groups and the direct exchange reaction between hole and hydrogen.[8–11] This has been proved by soft-X-ray emission spectroscopy (SXES) and soft-X-ray absorption spectroscopy (XAS).[8–11] In Sc-doped SrTiO$_3$[8,9] and In-doped CaZrO$_3$,[10] the hole state and the acceptor-induced level due to acceptor doping are observed at the top of the valence band and immediately above the Fermi level (E_F). The intensities of hole and acceptor-induced level decrease with hydrogen doping. This result suggests that hydrogen, which acts as donor, compensates the hole created at the top of the valence band by acceptor doping. The hydrogen-induced level is also created immediately below E_F. The energy separation between the hole and hydrogen-induced level coincides with the activation energy estimated from the transport properties. Similar phenomena might be expected in SrCe$_{1-x}$Y$_x$O$_{3-\delta}$. However, the electronic structure has not been clarified thus far.

In this paper, we present high-resolution SXES and soft-X-ray absorption spectroscopy XAS spectra of the protonic conductor, SrCe$_{1-x}$Y$_x$O$_{3-\delta}$. The SXES and XAS techniques can confirm the electronic structure of the bulk state,[11] because the mean free path of a soft-X-ray is very long compared with that of an electron. The SXES and XAS spectra, which have a clear selection rule regarding the angular momentum due to dipole transition, reflect the occupied partial-density-of-state (PDOS) and unoccuipied PDOS, respectively.[8] Thus, we observe the change of electronic structure with hydrogen doping by means of O $1s$ SXES and XAS techniques.

SrCe$_{1-x}$Y$_x$O$_{3-\delta}$ samples were sintered ceramics prepared by the solid-state reaction of SrCO$_3$, CeO$_2$, and Y$_2$O$_3$ at 1250°C, and pressed into cylinders of φ 13 mm $\times$ 80 mm, then sintered again in air at 1250°C for 20 h. The dopant concentrations were $x = 0$ and 0.05. The samples were confirmed as having a single phase with a perovskite structure by the powder X-ray diffraction analysis. The dry-annealed sample was prepared in an atmosphere of N$_2$ vapor pressure at 800°C in order to prevent hydrogen from entering the crystal. The wet-annealed sample was prepared in an atmosphere of saturated H$_2$O vapor at 20°C. The electrical conductivities of dry-annealed and wet-annealed samples were $1.0 \times 10^{-1}\,\Omega^{-1}\cdot\mathrm{cm}^{-1}$ and $1.2 \times 10^{-1}\,\Omega^{-1}\cdot\mathrm{cm}^{-1}$, respectively, at 400°C. The protonic conductivity of the wet-annealed SrCe$_{1-x}$Y$_x$O$_{3-\delta}$ sample was examined at temperatures below 500°C. The activation energies (E_A) of the dry-annealed and wet-annealed samples were 0.56 eV and 0.60 eV, respectively.

The XAS measurements were carried out at the revolver undulator beamline BL-19B at the Photon Factory (PF) of the High Energy Accelerator Organization (KEK), Tsukuba in Japan. High brightness with high resolution is realized using a varied line spacing plane grating monochromator. The SXES spectra were measured by a soft-X-ray emission spectrometer. The spectrometer used the Rowland circle geometry that consists of grating with a groove density of 300 lines/mm and a Cs-coated multichannel detector. The XAS spectra were measured by a Si photodiode. The total resolutions of SXES and XAS were approximately 0.4 eV and 0.1 eV, respectively. The incidence angle of soft-X-ray was sets as approximately 90° against the surface in order to avoid the surface effect.
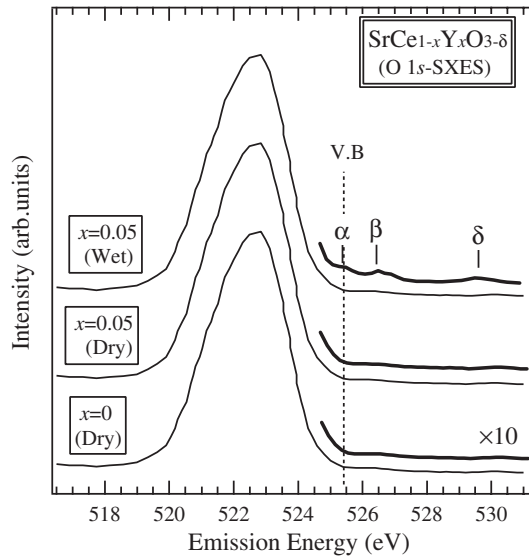
Fig. 1. O 1s SXES spectra of dry-annealed and wet-annealed SrCe$_{0.95}$Y$_{0.05}$O$_{3-\delta}$. As reference, the spectrum of undoped SrCeO$_3$ is also shown. The intensity of the emission energy region above 530.2 eV is expanded and shown as a thick line.

Fig. 2. O 1s XAS spectra of dry-annealed and wet-annealed SrCe$_{0.95}$Y$_{0.05}$O$_{3-\delta}$. As reference, the XAS spectrum of undoped SrCeO$_3$ is also shown. The intensity of the photon energy region above 535.5 eV is expanded and shown as a thick line.

Figure 1 shows the O 1s SXES spectra of dry-annealed and wet-annealed SrCe$_{0.95}$Y$_{0.05}$O$_{3-\delta}$. As a reference, the SXES spectrum of dry-annealed SrCeO$_{3-\delta}$ is also shown. The intensities of the SXES spectra are normalized by the beam current and measurement time. The clear selection rule of SXES is caused mainly within the same atomic species, because the core hole is strongly localized. For this reason, the O 1s SXES spectra reflect the O 2p PDOS. The obtained O 2p PDOS corresponds to the band structure in the valence band region, since the valence band of SrCeO$_3$ is mainly composed of O 2p.[12] The dashed line at ∼525.4 eV indicates the position of the top of the valence band (V.B). The bandwidth and peak positions do not differ in either spectra. This behavior is in good agreement with the results of the photoemission spectra in the valence band region.[12] The spectral intensity above the valence band is expanded by ten times and is shown as a thick line above the SXES spectrum in order to show the weak structure in the band-gap energy region clearly. There is no structure in the band-gap energy region of dry-annealed SrCeO$_{3-\delta}$ or SrCe$_{0.95}$Y$_{0.05}$O$_{3-\delta}$. Three features denoted by the α, β, and δ peaks are observed in the band-gap energy region of wet-annealed SrCe$_{0.95}$Y$_{0.05}$O$_{3-\delta}$.

Figure 2 shows the O 1s XAS spectra of dry-annealed and wet-annealed SrCe$_{0.95}$Y$_{0.05}$O$_{3-\delta}$. As a reference, the XAS spectrum of dry-annealed SrCeO$_{3-\delta}$ is also shown. The O 1s XAS spectra are normalized by the Sr 4d peak of the conduction band, though the peak is not shown in this figure. From the dipole selection rule, it is understood that the O 1s XAS spectra of Ce oxides correspond to transitions from O 1s to the O 2p character. The large band around 532 eV is mainly composed of the O 2p state hybridized with the unoccupied Ce 4f state. The spectral intensity below the threshold is expanded by ten times and is shown as a thick line above the XAS spectrum in order to show the electronic structure in the band-gap energy region. The XAS features below E_F correspond to the thermal excited structure from the
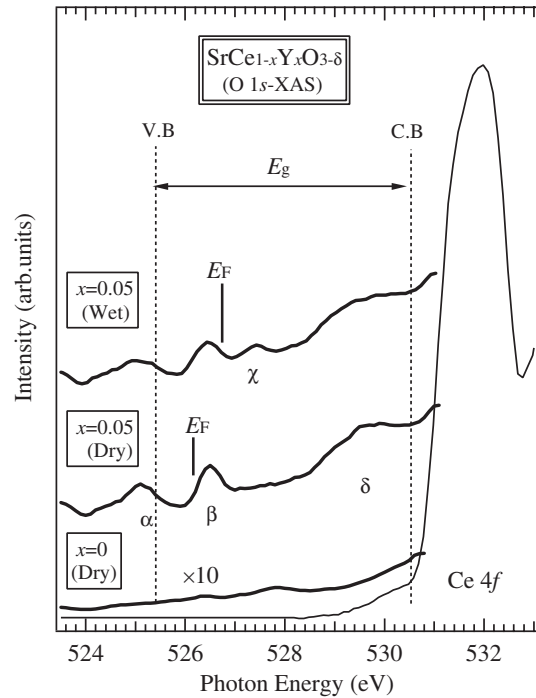
valence band. An arrow shows the top of the valence band. E_F is determined from the binding energy of the O 1s photoemission peak. E_F of dry-annealed SrCe$_{0.95}$Y$_{0.05}$O$_{3-\delta}$ is located at ∼0.5 eV above the top of the valence band. E_F of wet-annealed SrCe$_{0.95}$Y$_{0.05}$O$_{3-\delta}$ shifts to the conduction band side by approximately 0.6 eV. This shift of E_F expected from the rigid-band model indicates the existence of hydrogen, which acts as a donor in the crystal lattice.

In dry-annealed SrCe$_{0.95}$Y$_{0.05}$O$_{3-\delta}$, three features denoted by the α, β, and δ peaks are observed in the band-gap energy region. The apparent feature δ is considered to be a defect-induced level of the Ce 4f state, since the feature is located at the bottom of the Ce 4f conduction band (C.B). The similar defect-induced level has been reported in In-doped CaZrO$_3$ and Sc-doped SrTiO$_3$.[8–10] The feature α is assigned to holes created by Y doping at V.B., which is mainly composed of nonbonding O 2p states in the valence band. In the absorption spectra of the vacuum ultraviolet region, we have clarified that the band gap of Yb^{3+}-doped SrCeO$_3$ increases with increasing Yb^{3+} concentration.[12,13] The increase of the band gap contributes to the presence of holes created at the top of the valence band. The existence of the holes has been observed in the O 1s XAS spectra of Yb^{3+}-doped SrCeO$_3$.[9] This finding indicates that the filling of the acceptor is rigid-band-like. The same situation is expected in SrCe$_{0.95}$Y$_{0.05}$O$_{3-\delta}$. The feature β at E_F is assigned to the acceptor level, since it lies immediately above E_F. The existences of the hole and the acceptor level of dry-annealed SrCe$_{0.95}$Y$_{0.05}$O$_{3-\delta}$ are expected from the rigid-band model. In dry-annealed SrCeO$_3$, two broad features in the band-gap region are considered to contribute to the oxygen vacancies, though the origin has not been clarified thus far. In wet-annealed SrCe$_{0.95}$Y$_{0.05}$O$_{3-\delta}$, the intensities of the α, β, and δ

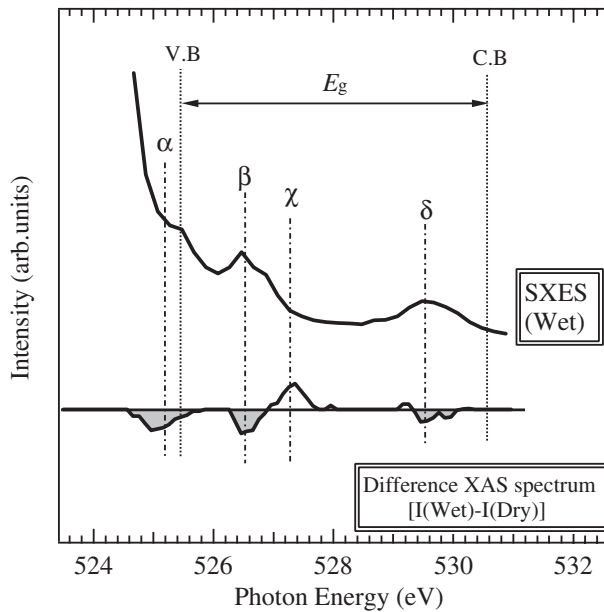Jpn. J. Appl. Phys. Vol. 42 (2003) Pt. 2, No. 10B

T. HIGUCHI *et al.*   L 1267

Fig. 3. Comparison between the O 1*s* SXES spectrum of wet-annealed $SrCe_{0.95}Y_{0.05}O_{3-\delta}$ and the difference spectrum obtained by subtracting the O 1*s* XAS spectrum of dry-annealed $SrCe_{0.95}Y_{0.05}O_{3-\delta}$ from that of wet-annealed $SrCe_{0.95}Y_{0.05}O_{3-\delta}$.

peaks decrease and the β peak splits into two features around E_F.

Figure 3 shows the comparison between the O 1*s* SXES spectrum of wet-annealed $SrCe_{0.95}Y_{0.05}O_{3-\delta}$ and the difference spectrum obtained by subtracting the O 1*s* XAS spectrum of dry-annealed $SrCe_{0.95}Y_{0.05}O_{3-\delta}$ from that of wet-annealed $SrCe_{0.95}Y_{0.05}O_{3-\delta}$. The difference XAS spectrum reflects the contribution of hydrogen to the O 2*p* DOS in the band-gap energy region. Comparing these two spectra, the energy positions of the three O 2*p* DOS are good agreement with those of the three hydrogen DOS, as indicated by the three vertical dashed lines (α, β and δ). These agreements indicate that oxygen bonds with hydrogen (O-H bond). The existence of the O-H bond is natural in the bulk state, since SXES and XAS are bulk sensitive measurements. The feature α corresponds to the O-H bond created at V.B. The feature β corresponds to the O-H bond near the Ce ion created at C.B. The feature β near E_F is considered to be the thermally excited hydrogen from feature α since the energy separation between V.B. and C.B. of feature β

matches with the activation energy estimated from the electrical transport measurement. Feature χ, which is located immediately above E_F of the wet-annealed $SrCe_{0.95}Y_{0.05}O_{3-\delta}$, is considered to be a hydrogen-induced level, though its origin has not been clarified thus far.

In conclusion, we have studied the electronic structure in the band-gap energy region of the hydrogenic conductor $SrCe_{0.95}Y_{0.05}O_{3-\delta}$ using SXES and XAS. The hydrogen DOS in the band-gap region was obtained by subtracting the XAS spectrum of dry-annealed $SrCe_{0.95}Y_{0.05}O_{3-\delta}$ from that of wet-annealed $SrCe_{0.95}Y_{0.05}O_{3-\delta}$. Three O 2*p* DOS in the band-gap region were also observed in wet-annealed $SrCe_{0.95}Y_{0.05}O_{3-\delta}$. The energy positions of the three hydrogen DOS are in agreement with those of O 2*p* DOS. These findings indicate that the O-H bond exists in the bulk state.

1) H. Iwahara, T. Esaka, H. Uchida and N. Maeda: Solid State Ionics **3/4** (1981) 359.
2) S. Shin, H. H. Huang, M. Ishigame and H. Iwahara: Solid State Ionics **40/41** (1990) 910.
3) H. Matsumoto, S. Hamajima and H. Iwahara: J. Electrochem. Soc. **148** (2001) D121.
4) T. Higuchi, T. Tsukamoto, N. Sata, K. Hiramoto, M. Ishigame and S. Shin: Jpn. J. Appl. Phys. **40** (2001) 4162.
5) T. Higuchi, T. Tsukamoto, S. Yamaguchi, N. Sata, K. Hiramoto, M. Ishigame and S. Shin: Jpn. J. Appl. Phys. **41** (2002) 6440.
6) K. Kobayashi, S. Yamaguchi and Y. Iguchi: Solid State Ionics **108** (1998) 355.
7) T. Yajima, K. Koide, N. Fukatsu, T. Ohashi and H. Iwahara: Sens. & Actuat. B **13/14** (1993) 697.
8) T. Higuchi, T. Tsukamoto, K. Kobayashi, S. Yamaguchi, Y. Ishiwata, N. Sata, K. Hiramoto, M. Ishigame and S. Shin: Phys. Rev. B **65** (2002) 33201.
9) T. Higuchi, T. Tsukamoto, N. Sata, M. Ishigame, K. Kobayashi, S. Yamaguchi and S. Shin: Solid State Ionics **154–155** (2002) 735.
10) T. Higuchi, S. Yamaguchi, K. Kobayashi, T. Takeuchi, S. Shin and T. Tsukamoto: Jpn. J. Appl. Phys. **41** (2002) L938.
11) T. Higuchi, T. Tsukamoto, S. Yamaguchi, N. Sata, M. Ishigame and S. Shin: Jpn. J. Appl. Phys. **42** (2003) 3526.
12) N. Sata, H. Yugami, Y. Akiyama, T. Hattori, S. Yamaguchi and M. Ishigame: Solid State Ionics **121** (1999) 321.
13) T. Higuchi, T. Tsukamoto, N. Sata, T. Hattori, M. Ishigame and S. Shin: in preparation for publication.